

Effect of Mechanical Stress on Rheumatoid Arthritis of the Temporomandibular Joint: a Morphological and Histological Evaluation

Kohei Nagai

Tokyo Dental College Department of Orthodontics <https://orcid.org/0000-0002-9174-6646>

Takenobu Ishii (✉ ishiit@tdc.ac.jp)

Department of Orthodontics, Tokyo Dental College <https://orcid.org/0000-0003-0654-1521>

Yasushi Nishii

Tokyo Dental College Department of orthodontics

Research article

Keywords: temporomandibular joint, rheumatoid arthritis, mechanical stress, γ δ T cell

Posted Date: July 14th, 2021

DOI: <https://doi.org/10.21203/rs.3.rs-658268/v1>

License:  This work is licensed under a Creative Commons Attribution 4.0 International License.

[Read Full License](#)

Abstract

Background

Rheumatoid arthritis of the temporomandibular joint (TMJ-RA) has been reported to have a larger incidence range than systemic rheumatoid arthritis (RA). The presence or absence of mechanical stress (MS) is considered a factor in this. In this study, we hypothesized that TMJ-RA develops or worsens when excessive MS is applied to the temporomandibular joint of RA mouse models. We aimed to clarify the relationship between TMJ-RA and MS through morphological and histological evaluation.

Methods

Collagen antibody-induced arthritis (CAIA) was induced in male DBA/1JNCrlj 9–12 weeks old mice by administering Type II collagen antibody and lipopolysaccharide to produce RA model mice. MS was applied to the mandibular condyle. The group was separated into non-RA (control group (N = 5) and MS group (N = 5)), and RA group (CAIA group (N = 5) and CAIA MS group (N = 5)). To confirm the morphological changes in the mandibular condyle, micro-CT imaging was performed. Histological evaluation of the TMJ was performed by hematoxylin and eosin staining for condylar cartilage cell layer thickness, Safranin O staining for proteoglycans, and tartrate-resistant acidic phosphatase staining for osteoclast count. Immunohistochemical evaluation was performed to assess the localization of cartilage destruction enzymes using ADAMTS-5 (a disintegrin and metalloproteinase with thrombospondin motifs) antibody. Additionally, CD3 (cluster of differentiation), CD45, and $\gamma\delta$ TCR (T cell receptor) antibodies were used to localize and identify the type of lymphocytes.

Results

In the CAIA MS model, a three-dimensional analysis of the temporomandibular joint by microcomputer tomography showed a crude change in the surface of the mandibular condyle. Histological examination revealed a decrease in the chondrocyte layer width and an increase in the number of osteoclasts in the mandibular condyle. T cell accumulation was observed, and $\gamma\delta$ T cell involvement was confirmed.

Conclusions

In the CAIA model, the TMJ was less sensitive to the initiation of RA. However, the results suggested that it was exacerbated by MS, and that $\gamma\delta$ T cells may be involved in TMJ-RA.

Background

Rheumatoid arthritis (RA) is an unexplained autoimmune disease with a 1% prevalence worldwide. Chronic inflammation of the joints and synovial hyperplasia, known as pannus, are observed, as well as

cartilage and bone destruction by inflammatory cytokines. The detailed cause of RA has not yet been fully elucidated (1). The most common sites of RA are the peripheral limb joints (knees, elbows, fingers) and the temporomandibular joint (TMJ). Previous reports have shown that 4–85% of RA patients develop RA in the TMJ (2, 3, 4). In this way, the morbidity range is wide; unlike RA in the limb joints, the pathogenic mechanism of RA in the TMJ (TMJ-RA) is still unknown.

TMJ-RA first causes degradation of proteoglycan and softening and degeneration of the mandibular condylar cartilage, followed by destruction of the subchondral bone and bone resorption by osteoclasts (2). Inflammatory cells, such as macrophages, infiltrate the synovial tissue and form pannus. They then release a chemical mediator, destroying the joint and causing pain (2, 3). In particular, tumor necrosis factor alpha (TNF- α) and interleukin 1 beta (IL-1 β) are associated with RA etiology (4, 5, 6). They cause excessive production and secretion of proteolytic enzymes such as matrix metalloproteinase (MMP) and A disintegrin and metalloproteinase with thrombospondin motifs (ADAMTS) in synovial fibroblasts, and deform the mandibular condyle cartilage. These degenerative changes can cause joint dysfunction, fibrous and bony ankylosis, occlusal-facial malformations, and occlusal inconsistencies. Therefore, early diagnosis and treatment are required (7).

Several RA animal models have been established for the analysis (8). In particular, collagen-induced arthritis (CIA) and collagen antibody-induced arthritis (CAIA) mice share many morphological similarities with human RA, such as the production of autoantibodies to Type II collagen (9), and are therefore often used as RA models. However, most studies have focused on the knee and hind limb joints, and TMJ-RA has not yet been reported in detail. RA models and human RA clinical symptoms suggest that limb joint RA is exacerbated by overloading (10, 11), and it has been reported that overloading the mandibular condyle also causes osteoarthritis-like cartilage resorption (12, 13).

Unlike the joints of the extremities, made of hyaline cartilage, which is constantly loaded, the TMJ contains fibrocartilage, a tissue that is loaded only during functions such as mastication (14). Therefore, the TMJ may be more vulnerable to overload than the limb joints. In this study, we devised a method for overloading by pushing the mandibular condyle posteriorly according to this hypothesis.

Therefore, the purpose of this study was to clarify the effect of load on the TMJ on the onset of RA by using the CAIA mouse model and to elucidate the causes of TMJ-RA.

Methods

Mice

Animal experiments were approved by the Ethics Committee of Tokyo Dental College (Ethics Application Number: 203102). Male DBA/1JNCrlj mice were bred until 7–8 weeks of age (Charles River, Yokohama, Japan) under standard environmental conditions and were given free access to solid feed and tap water. The mice in the experiment were divided into non-RA group (a control group [N = 5] and a mechanical stress [MS] group [N = 5]) and RA group (a CAIA group [N = 5] and a CAIA MS group [N = 5]). The mice were

anesthetized and a metal plate (product number: 21700BZZ00197000, TOMY INTERNATIONAL INC., Tokyo) was bonded to the posterior surface of the maxillary portal teeth with dental composite resin to a basal thickness of 2 mm to induce an imbalanced occlusion. After anesthesia, the control and CAIA groups did not wear the device. Fourteen days after the start of the experiment, after induction of anesthesia with an inhalant anesthetic (sevoflurane), the mice were euthanized by intraperitoneal overdose of 150 mg/kg pentobarbital sodium, and samples were collected (Fig. 1A, B).

CAIA production

Nine- to 12-week-old mice (N = 20) were injected intraperitoneally with 1.5 mg of ArthroGen-CIA® Arthritogenic Monoclonal Antibody Cocktail (Condrex Inc, WA, USA). Three days after antibody administration, 25 µg of LPS (Lipopolysaccharide) was injected intraperitoneally to induce CAIA (CAIA and CAIA MS group) (9,15). The control and MS groups were injected intraperitoneally with phosphate-buffered saline.

Evaluation of arthritis

The severity of arthritis was blindly scored on a scale of 0 to 4 as follows: 1 (mild swelling confined to the ankle or tarsal joint), 2 (mild swelling extending to the center of the foot), 3 (moderate swelling over the metatarsal joints), and 4 (severe swelling including the ankles, feet, and fingers). The scores of all four feet were summed to generate an arthritis score with a maximum value of 16 (16).

Evaluation of inflammation by histological staining of the knee joint

The mice were euthanized 14 days after the injection of anti-Type II collagen antibody, and the knee joints were fixed with 10% formaldehyde (Wako Pure Chemical Corporation, Japan) for 2 days. The knee joints were then decalcified in 10% ethylenediaminetetraacetic acid (EDTA [MUTO PURE CHEMICALS CO, LTD. Japan]) at 4°C for 30 days and embedded in paraffin. The knee joint tissues were sliced into 4 µm sections and subjected to hematoxylin and eosin (HE) and Safranin O staining to evaluate the morphological changes in the femur and tibia and the staining of proteoglycans in the chondrocyte layer.

Measurement of inflammatory cytokines in blood

All mice were standardized by restricting their eating and drinking for three hours prior to blood collection. Blood was collected using a 5 mm Goldenrod Animal Lancet (MEDI Point NY, USA) and bled using the submandibular bleeding method. Blood was collected in BD Microtina microcentrifuge tubes (365967 Fisher Scientific Pittsburgh, PA) with coagulant accelerator and serum separator and allowed to coagulate at 4°C for 30 minutes. It was then centrifuged at 13,000 rpm for 10 mins and the serum was collected and stored at -20°C. The Mouse IL-1β/IL-1F2 Immunoassay ELISA kit (Catalog Number MLB00C Quantikine® ELISA MN, USA) was used to evaluate the serum IL-1β levels in mice. The assay was performed in the non-RA and RA groups (n = 9).

Morphological evaluation by micro-computed tomography

The dimensions of bone destruction were measured and analyzed using microcomputer tomography (μ CT) imaging after euthanasia (R_mCT, RIGAKU, Tokyo, Japan). The sample was irradiated with X-rays with a tube voltage of 90 kV and a tube current of 150 mA. The shooting time was 2 mins, the shooting magnification was 10 times, and the voxel size was 20 \times 20 \times 20 μ m. For evaluation, μ CT images were constructed three-dimensionally using the bone structure analysis software TRI/3D-BON (Ratoc System Engineering Co. Ltd., Japan), and the mandibular condyle length and width were measured (17) (Fig. 1.C). The percentage of the crude area was measured using the ImageJ software (National Institutes of Health, Bethesda, MD) from the ratio of the number of pixels in the crude area of the mandibular condyle to the number of pixels in the entire mandibular condyle image. The area of interest was from the crown of the mandibular condyle to the rearmost part (18).

Histopathological analysis of the mandibular condyle

After euthanasia, the heads were fixed with 10% formaldehyde for 2 days. They were then decalcified in 10% EDTA at 4°C for 30 days and embedded in paraffin. The TMJ tissues were sliced into 4 μ m sections. The TMJ was stained with HE staining to evaluate mandibular condyle morphology and to measure the average TMJ condylar cartilage cell layer thickness in the mid-coronal portion of the mandibular condylar head of five mice in each group. Additionally, the staining of proteoglycans in the mandibular condyle was evaluated by staining with Safranin O. Tartrate-resistant acid phosphatase (TRAP) staining was then performed to evaluate osteoclast differentiation in subchondral bone. TRAP activity was measured according to the method given by Shirakura M et al. (19), and TRAP-positive cells with three or more nuclei were counted as osteoclasts using a TRAP staining kit (Sigma, St. Louis, MO, USA).

Evaluation of immunohistochemistry of the mandibular condyle

After deparaffinizing the sections of each group, we performed antigen retrieval with the agent ImmunoSaver Antigen Retriever (Electron Microscopic Sciences, Hatfield, PA), and blocking with 1% bovine serum albumin. Immunofluorescence staining was performed using ADAMTS (a disintegrin and metalloproteinase with thrombospondin motifs); -5 rabbit polyclonal antibody (abcam, Cambridge, MA, USA), CD (cluster of differentiation) 3 rabbit polyclonal antibody (my biosource Inc., CA, USA), CD45 rat monoclonal antibody (my biosource Inc., CA, USA), and $\gamma\delta$ TCR (T cell receptor) mouse monoclonal antibody (Santa Cruz Biotechnology, TX, USA) were used as the primary antibodies. Secondary antibodies were Alexa Fluor 546 Donkey Anti-Rabbit IgG (Thermo Fisher Scientific, US) to detect ADAMTS-5, and CD45, γ δ TCR, and Alexa Fluor 647 Goat Anti-Rat IgG (Thermo Fisher Scientific, US) to detect CD3. Nuclear staining was performed using stain solution Hoechst 33342 (Thermo Fisher Scientific, US). The number of cells was measured using the ImageJ software.

Statistical analysis

SPSS 17.0 (SPSS Inc. CHI, USA) was used for statistical analyses. For in-group comparisons, multiple comparisons were performed using the Tukey-Kramer test. For comparisons with the control group,

multiple comparisons were performed using Dunnett's test. Comparisons between two groups were made using Student's t test. The level of significance was set at $P < 0.05$ (*).

Results

Evaluation of arthritis in CAIA

All mice injected with the collagen antibody cocktail developed inflammatory arthritis after LPS administration. The arthritis score was 0 in the non-RA group, and 12 in the RA group on the 6th day of administration, and thereafter maintained a stable score of about 14 until sacrifice (Fig. 2A, B). The localization of inflammatory cells in knee osteoarthritis and their effect on the chondrocyte layer were investigated using HE and Safranin O staining. As a result, in the RA group, infiltration of inflammatory cells was observed in the joint cavity, and a defect in the surface layer of the femur and proteoglycan erosion in the chondrocyte layer were observed, compared with the non-RA group (Fig. 2C). In the RA group, the systemic concentration of the pro-inflammatory cytokine IL1- β increased approximately 1.5-fold compared to the non-RA group (Fig. 2D).

Evaluation of mandibular condyle morphology in μ CT

A morphological evaluation of the mandibular condyle was performed using μ CT. The mandibular condyle length and width were measured as shown in Fig. 1C, but no significant change was found in the width diameter of each group (Fig. 3A). The morphological evaluation of each group revealed changes in the posterior part of the mandibular condyle and signs of bone destruction in the CAIA MS group (Fig. 3B). Moreover, the crude area increased approximately 1.5-fold in the CAIA MS group compared with the control group (Fig. 3C).

Histological evaluation of mandibular condyle morphology

The mandibular condyle HE staining showed no clear morphological changes in each group compared to the control group (Fig. 4A(a-d)). In the HE staining, the CAIA group did not show abnormal synovial proliferation or accumulation of inflammatory cells (Fig. 4A(c)). In the CAIA MS group, accumulation of inflammatory cells in the TMJ cavity was observed (Fig. 4A(d), Fig. 4B). Additionally, the mean TMJ condyle cartilage cell layer thickness in the CAIA MS group was significantly thinner than that in the control group (Fig. 4C). Safranin O staining showed decreased staining of proteoglycans in the MS and CAIA MS groups compared to the control group (Fig. 4A(e-h)). The number of TRAP-positive cells in the subchondral bone was higher in each group compared with the control group. (Fig. 4A(i-l)). The total number of osteoclasts measured by TRAP-positive cell counting increased significantly in all experimental groups compared to the control group, especially in the CAIA MS group, in which the number of osteoclasts increased by approximately 2-fold compared to the control group (Fig. 4D). The expression of ADAMTS-5, a chondrocyte-destroying enzyme, was also higher in the chondrocyte layer of the CAIA MS group (Fig. 4A(n-p)).

Confirmation of lymphocyte localization in TMJ by immunofluorescent staining

The localization of lymphocytes was confirmed by immunofluorescence staining. Accumulated B cell expression was observed in the subchondral bone of each group. Accumulated T cell expression was hardly observed in the control and MS groups. However, in the CAIA and CAIA MS groups, the expression of accumulated T cells in the subchondral bone was observed (Fig. 5A). There was no significant difference in the expression of B cells in each group (Fig. 5B). The localization of T cells in the CAIA MS group was approximately 2-fold higher than that in the control group (Fig. 5C).

Confirmation of localization of $\gamma\delta$ T cells in TMJ by immunofluorescent staining

There was little localization of $\gamma\delta$ T cells in the control, MS, and CAIA groups. However, in the CAIA MS group, $\gamma\delta$ T cells were mostly localized in the subchondral bone (Fig. 6A). The localization of $\gamma\delta$ T cells in the CAIA MS group was approximately 6-fold higher than that in the control group (Fig. 6B).

Discussion

Creating a CAIA mouse model

In this experiment, CAIA was developed with reference to the report by Nandakumar et al. (15). In general, because of the action of female hormones, female mice may not be suitable for accurate studies on bone metabolism or joint inflammation and bone tissue destruction; therefore, male mice were used in this experiment (20, 21). CAIA was used because it shares many morphological similarities with human RA, including the production of autoantibodies to Type II collagen. The CAIA group showed a significant increase in the arthritis score and swelling of the limb joints compared with the control group.

Furthermore, HE staining showed inflammatory cell proliferation in the knee joint space. Safranin O staining showed a decrease in proteoglycans. This is consistent with a report that the CAIA model causes extensive infiltration of subsynovial tissue by inflammatory cells, cell infiltration into the joint space, and significant cartilage destruction (9). Furthermore, there was an increase in the concentration of IL-1 β in the blood. These results confirmed the existence of systemic arthritis inflammation and proved that the CAIA mouse model was correctly generated.

Effects of excessive MS on the mandibular condyle in the CAIA mouse model

In the RA model, limb joints show swelling, erythema, and synovial proliferation, but clinical signs in the TMJ are generally unclear; therefore, attempts to investigate the RA model of the TMJ have been made recently. In a study using a cartilage proteoglycan (PG)-induced arthritis (PGIA) mouse model, increased ADAMTS in the TMJ was observed, but structural damage was only observed in the TMJ of mice with

severe arthritis symptoms (22). In another study using the K/BxN model of spontaneous inflammation, increased expression of vascular endothelial growth factor and IL-17, and decreased expression of osteoprotegerin were observed in the limb joints, but not in the TMJ (23). In the same study with the K/BxN mouse model, the enlargement of the upper joint cavity in arthritic mice was confirmed by Magnetic Resonance Imaging, and only cartilage detachment of the TMJ surface was observed (24). In the present study, although the CAIA group showed increased osteoclast differentiation, there was no significant thinning of the chondrocyte layer or localization of lymphocytes. These results suggest that the TMJ is a less primary target for inflammation than the limbic joints in the RA model. However, in the CAIA MS group, ADAMTS-5 was strongly observed, the chondrocyte layer was thinned, and lymphocytes increased in localization. Therefore, it can be inferred that overloading of the TMJ is a factor in the development of TMJ-RA. Functional occlusal loading on the TMJ (by forced unilateral or anterior occlusion) has been shown to lead to worsening of TMJ arthritis (25,26). Therefore, overloading the mandibular condyle may accelerate the degeneration of the mandibular condyle cartilage, and overloading the TMJ may be an important factor for the development of inflammation in the TMJ in the RA model.

The metal plate device used in the present study as a method of applying MS to the mandibular condyle applied excessive MS to the TMJ, demonstrating that it can induce TMJ-RA in CAIA mice. It has been reported that TMJ osteoarthritis-like changes occurred when a resin block was attached to a rats maxillary horn teeth and the mandible was pushed backward (19). Therefore, we designed a similar device for the mouse model. Unlike the TMJ, which is composed of hyaline cartilage, the mandibular condyle cartilage is composed of fibrocartilage derived from periosteal tissue, so the size and characteristics of the tissue are adjusted to adapt to changes in load (27). As the device we used in this study used a metal plate for the occlusal part, it did not wear because of occlusion, and its thickness remained constant during the device wearing period. Therefore, as it can be regarded that a stable overload was applied to the mandibular condyle, this method is considered to be very useful for establishing a load on the TMJ in mice.

Among all the experimental groups examined in this study, TMJ-RA showed worsening of pathology in the group that combined excessive MS and systemic inflammation (CAIA MS group). Therefore, we confirmed that excessive MS worsens the pathology of the TMJ in CAIA mice.

Involvement of $\gamma\delta$ T cells in the mandibular condyle in CAIA mouse model

The CAIA mouse model is not affected by lymphocytes when inflammation develops. However, exacerbation of arthritis due to Type II collagen-reactive T cells in limb joints has been reported in CAIA (28, 29). In this study, T cell localization was observed in the subchondral bone of the CAIA MS group. Furthermore, the localization of $\gamma\delta$ T cells, which have the smallest number among T cells, was also observed. $\gamma\delta$ T cells produce IL-17 and are known to be an important factor in cancer research (30). IL-17 is a cytokine that induces the expression of various pro-inflammatory cytokines and chemokines in a

wide variety of cells (31). $\gamma\delta$ T cells have also been shown to be associated with RA (32). It has been reported that the number of IL-17-producing cells in mouse femoral bone marrow also increases in CAIA mice (33). Furthermore, it has been reported that $V\gamma 4 / V\delta 4 + \gamma\delta$ T cells, one of the $\gamma\delta$ T cell subsets, produce IL-17, with localization in the synovial membrane and peripheral blood in CIA mice (34). However, because there is no report that $\gamma\delta$ T cells are involved in TMJ-RA, we investigated this and found that they were involved. Therefore, T cells increase in TMJ-RA by applying MS, and among them, $\gamma\delta$ T cells increase. Moreover, it is suggested that this may be aggravated by the production of IL-17.

However, this experiment could not clarify why $\gamma\delta$ T cells show increased localization in the TMJ. Isopentenyl pyrophosphate (IPP) is a factor that activates $\gamma\delta$ T cells (35). However, IPP is an intermediate product of the intracellular mevalonate pathway, which is difficult to quantify and has not been identified. Therefore, further research on quantification methods is needed.

Conclusion

The TMJ is less susceptible to inflammation in RA. However, MS exacerbates the disease. The findings suggested that $\gamma\delta$ T cells are involved in TMJ-RA as a causal factor. In the future, it is considered that new treatments targeting $\gamma\delta$ T cells may be required for TMJ-RA.

Abbreviations

RA: rheumatoid arthritis

TMJ: temporomandibular joint

CIA: collagen-induced arthritis

CAIA: collagen antibody-Induced arthritis

MS: mechanical stress

μ CT: microcomputer tomography

EDTA: ethylenediaminetetraacetic acid

HE: hematoxylin and eosin

TRAP: tartrate-resistant acidic phosphatase

ADAMTS: a disintegrin and metalloproteinase with thrombospondin motifs

CD: cluster of differentiation

TCR: T cell receptor

IPP: isopentenyl pyrophosphate

Declarations

Ethics approval and consent to participate

Animal experiments were approved by the Ethics Committee of Tokyo Dental College (Ethics Application Number: 203102).

Consent for publication

Not applicable.

Availability of data and materials

Relevant files of this work will be shared on request.

Competing interests

Not applicable.

Funding

The work was supported by the Department of Orthodontics, Tokyo Dental College.

Authors' contributions

KN along with TI designed and performed the experiments and conducted data analysis. KN wrote the manuscript. TI and YN contributed in manuscript editing. All authors read and approved the final manuscript.

Acknowledgments

Not applicable.

References

1. Smolen JS, Aletaha D, McInnes IB. Rheumatoid arthritis. *Lancet*. 2016;388(10055):2023–38. doi : org/10.1016/S0140-6736(16)30173-8
2. Liu WW, Xu ZM, Li ZQ, Zhang Y, Han B. RANKL, OPG and CTR mRNA expression in the temporomandibular joint in rheumatoid arthritis. *Exp Ther Med*. 2015;10(3):895–900. doi : 10.3892/etm.2015.2629
3. Strand V, Kavanaugh AF. The role of interleukin-1 in bone resorption in rheumatoid arthritis. *Rheumatology (Oxford)*. 2004;43 Suppl 3:10–6. doi : 10.1093/rheumatology/keh202

4. Ahmed N, Petersson A, Catrina AI, Mustafa H, Alstergren P. Tumor necrosis factor mediates temporomandibular joint bone tissue resorption in rheumatoid arthritis. *Acta Odontol Scand*. 2015;73(3):232–40. doi : 10.3109/00016357.2014.994561
5. Kagari T, Doi H, Shimozato T. The Importance of IL-1 β and TNF- α , and the Noninvolvement of IL-6, in the Development of Monoclonal Antibody-Induced Arthritis. *J Immunol*. 2002;169(3):1459–66. doi : 10.4049/jimmunol.169.3.1459
6. Nie H, Zheng Y, Li R, Guo TB, He D, Fang L, et al. Phosphorylation of FOXP3 controls regulatory T cell function and is inhibited by TNF- α in rheumatoid arthritis. *Nat Med*. 2013;19(3):322–8. doi : 10.1038/nm.3085
7. Lin YC, Hsu ML, Yang JS, Liang TH, Chou SL, Lin HY. Temporomandibular joint disorders in patients with rheumatoid arthritis. *J Chinese Med Assoc*. 2007;70(12):527–34. doi : 10.1016/S1726-4901(08)70055-8
8. Caplazi P, Baca M, Barck K, Carano RAD, DeVoss J, Lee WP, et al. Mouse Models of Rheumatoid Arthritis. *Vet Pathol*. 2015;52(5):819–26. doi : 10.1177/0300985815588612
9. Terato K, Hasty KA, Reife RA, Cremer MA, Kang AH, Stuart JM. Induction of arthritis with monoclonal antibodies to collagen. *J Immunol*. 1992;148:2103–8.
10. Cambré I, Gaublomme D, Burssens A, Jacques P, Schryvers N, De Muynck A, et al. Mechanical strain determines the site-specific localization of inflammation and tissue damage in arthritis. *Nat Commun*. 2018;9(1):1–14. doi : 10.1038/s41467-018-06933-4
11. Koh JH, Jung SM, Lee JJ, Kang KY, Kwok SK, Park SH, et al. Radiographic structural damage is worse in the dominant than the non-dominant hand in individuals with early rheumatoid arthritis. *PLoS One*. 2015;10(8):1–13. doi : 10.1371/ journal.pone.0135409
12. Sierra H, Cordova M, Chen CSJ, Rajadhyaksha M. Confocal imaging-guided laser ablation of basal cell carcinomas: An ex vivo study. *J Invest Dermatol*. 2015;135(2):612–5. doi : 10.1016/j.joca.2008.05.021.
13. Ikeda Y, Yonemitsu I, Takei M, Shibata S, Ono T. Mechanical loading leads to osteoarthritis-like changes in the hypofunctional temporomandibular joint in rats. *Arch Oral Biol*. 2014;59(12):1368–76. doi : org/10.1016/j.archoralbio.2014.08.010
14. Ghassemi Nejad S, Kobezda T, Tar I, Szekanecz Z. Development of temporomandibular joint arthritis: The use of animal models. *Jt Bone Spine*. 2017;84(2):145–51. doi : 10.1111/1756-185X.13486
15. Nandakumar KS, Holmdahl R. Efficient promotion of collagen antibody induced arthritis (CAIA) using four monoclonal antibodies specific for the major epitopes recognized in both collagen induced arthritis and rheumatoid arthritis. *J Immunol Methods*. 2005;304(1–2):126–36. doi : 10.1016/j.jim.2005.06.017
16. Bonnefoy F, Daoui A, Valmary-Degano S, Toussiroit E, Saas P, Perruche S. Apoptotic cell infusion treats ongoing collagen-induced arthritis, even in the presence of methotrexate, and is synergic with anti-TNF therapy. *Arthritis Res Ther*. 2016;18(1):1–13. doi : org/10.1186/s13075-016-1084-0

17. Crossman J, Alzaheri N, Abdallah MN, Tamimi F, Flood P, Alhadainy H, et al. Low intensity pulsed ultrasound increases mandibular height and Col-II and VEGF expression in arthritic mice. *Arch Oral Biol.* 2019;104(2):112–8. doi : org/10.1016/j.archoralbio.2019.05.032
18. Katsumata Y, Kanzaki H, Honda Y, Tanaka T, Yamaguchi Y, Itohiya K, et al. Single local injection of epigallocatechin gallate-modified gelatin attenuates bone resorption and orthodontic tooth movement in mice. *Polymers (Basel).* 2018;10(12):1384. doi : org/10.3390/polym10121384
19. Shirakura M, Tanimoto K, Eguchi H, Miyauchi M, Nakamura H, Hiyama K, et al. Activation of the hypoxia-inducible factor-1 in overloaded temporomandibular joint, and induction of osteoclastogenesis. *Biochem Biophys Res Commun.* 2010;393(4):800–5. doi : org/10.1016/j.bbrc.2010.02.086
20. Yoneda T, Ishimaru N, Arakaki R, Kobayashi M, Izawa T, Moriyama K, et al. Estrogen deficiency accelerates murine autoimmune arthritis associated with receptor activator of nuclear factor- κ B ligand-mediated osteoclastogenesis. *Endocrinology.* 2004;145(5):2384–91. doi : 10.1210/en.2003-1536
21. Sekiguchi Y, Mano H, Nakatani S, Shimizu J, Wada M. Effects of the Sri Lankan medicinal plant, *Salacia reticulata*, in rheumatoid arthritis. *Genes Nutr.* 2010;5(1):89–96. doi : 10.1007/s12263-009-0144-3
22. Ghassemi-Nejad S, Kobezda T, Rauch TA, Matesz C, Glant TT, Mikecz K. Osteoarthritis-like damage of cartilage in the temporomandibular joints in mice with autoimmune inflammatory arthritis. *Osteoarthr Cartil.* 2011;19(4):458–65. doi : org/10.1016/j.joca.2011.01.012
23. Safi S, Frommholz D, Reimann S, Götz W, Bourauel C, Neumann AL, et al. Comparative study on serum-induced arthritis in the temporomandibular and limb joint of mice. *Int J Rheum Dis.* 2019;22(4):636–45. doi : 10.1111/1756-185X.13486
24. Kuchler-Bopp S, Mariotte A, Strub M, Po C, De Cauwer A, Schulz G, et al. Temporomandibular joint damage in K/BxN arthritic mice. *Int J Oral Sci.* 2020;12(1). doi : org/10.1038/s41368-019-0072-z
25. Liu YD, Liao LF, Zhang HY, Lu L, Jiao K, Zhang M, et al. Reducing dietary loading decreases mouse temporomandibular joint degradation induced by anterior crossbite prosthesis. *Osteoarthr Cartil.* 2014;22(2):302–12. doi : 10.1016/j.joca.2013.11.014
26. Liu YD, Yang HX, Liao LF, Jiao K, Zhang HY, Lu L, et al. Systemic administration of strontium or NBD peptide ameliorates early stage cartilage degradation of mouse mandibular condyles. *Osteoarthr Cartil.* 2016;24(1):178–87. doi : 10.1016/j.joca.2015.07.022
27. Robinson JL, Cass K, Aronson R, Choi T, Xu M, Bottenbaum R, et al. Sex differences in the estrogen-dependent regulation of temporomandibular joint remodeling in altered loading. *Osteoarthr Cartil.* 2017;25(4):533–43. doi : 10.1016/j.joca.2016.11.008.
28. Nandakumar KS, Bäcklund J, Vestberg M, Holmdahl R. Collagen type II (CII)-specific antibodies induce arthritis in the absence of T or B cells but the arthritis progression is enhanced by CII-reactive T cells. *Arthritis Res Ther.* 2004;6(6): R544–R550. doi : 10.1016/j.jim.2005.06.017

29. Mitamura M, Nakano N, Yonekawa T, Shan L, Kaise T, Kobayashi T, et al. T cells are involved in the development of arthritis induced by anti-type II collagen antibody. *Int Immunopharmacol.* 2007;7(10):1360–8. doi : 10.1016/j.intimp.2007.05.021
30. Zou C. $\gamma\delta$ T cells in cancer immunotherapy. *Oncotarget.* 2017;8(1):8900–9. doi : 10.1038/cr.2016.151
31. Weaver CT, Hatton RD, Mangan PR, Harrington LE. IL-17 family cytokines and the expanding diversity of effector T cell lineages. *Annu Rev Immunol.* 2007;25:821–52. doi : 10.1146/annurev.immunol.25.022106.141557
32. Bank I. The Role of Gamma Delta T Cells in Autoimmune Rheumatic Diseases. *Cells.* 2020;9(2):462. doi : org/10.3390/cells9020462
33. Grahnmemo L, Andersson A, Nurkkala-Karlsson M, Stubelius A, Lagerquist MK, Svensson MND, et al. Trabecular bone loss in collagen antibody-induced arthritis. *Arthritis Res Ther.* 2015;17(1):1–6. doi : org/10.1186/s13075-015-0703-5
34. Roark CL, French JD, Taylor MA, Bendele AM, Born WK, O'brien RL. $\gamma\delta$ T cells clonally expand, produce IL-17, and are pathogenic in collagen-induced arthritis. *J Immunol.* 2007;179(8):5576–83.
35. Wang RN, Wen Q, He WT, Yang JH, Zhou CY, Xiong WJ, et al. Optimized protocols for $\gamma\delta$ T cell expansion and lentiviral transduction. *Mol Med Rep.* 2019;19(3):1471–80. doi : 10.3892/mmr.2019.9831

Figures

Fig 2.

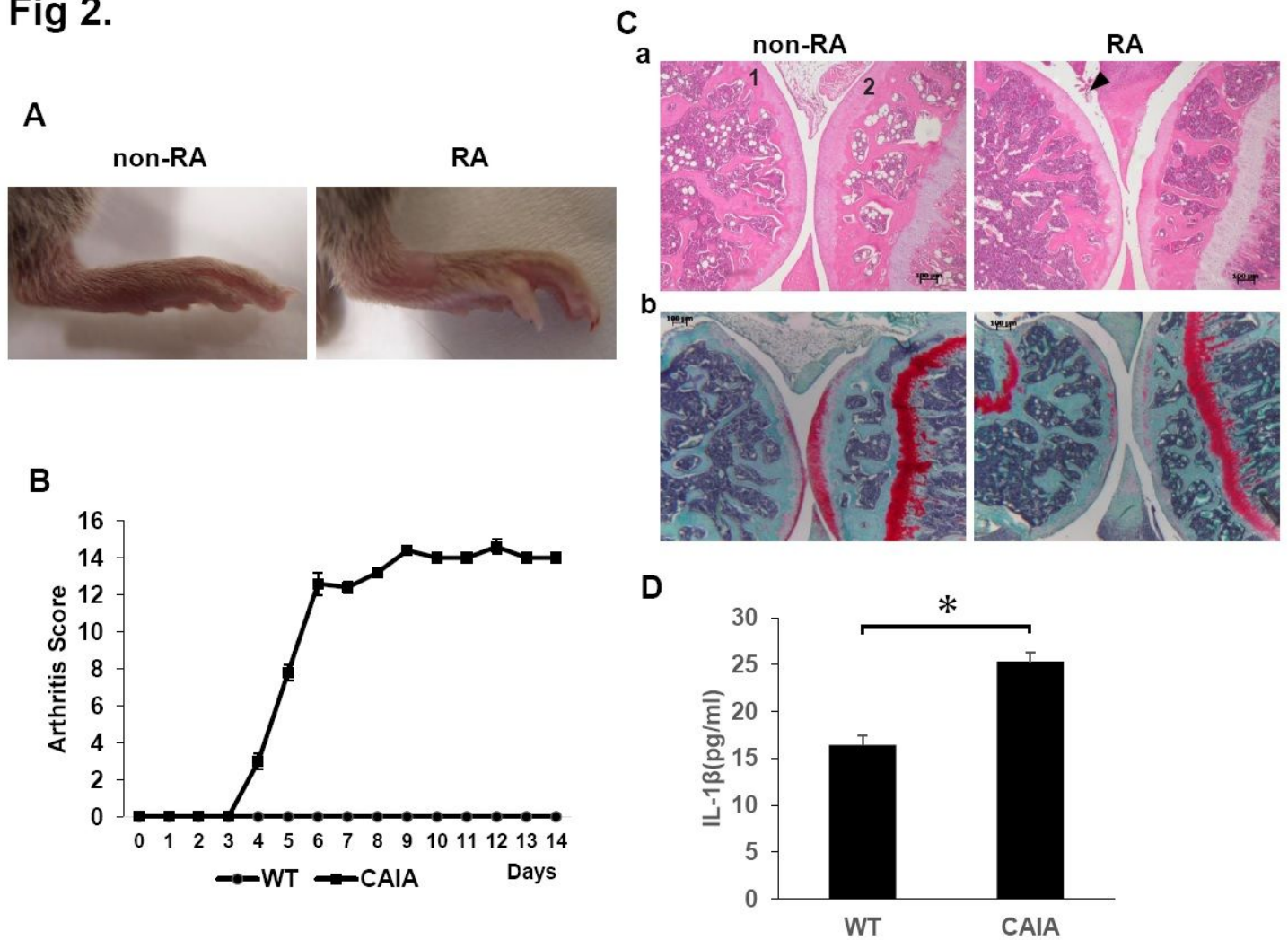


Figure 2

Inflammation evaluation. A. Clinical photographs of hind legs of control non-RA group and RA group mice. Swelling of the ankle was observed in the RA group. (Score 3) B. Clinical severity of arthritis in non-RA group and RA group after collagen antibody cocktail injection. Severity of arthritis in each foot was scored from 0 (no swelling) to 4 (erythema and severe swelling of the entire tarsal joint), and the total of 4 feet (0–16). In the RA group, the score was about 12 on day 6 of antibody administration. * $P < 0.05$. C. Histological analysis of the hind paw of each group on day 14. The knee joint was stained with hematoxylin and eosin a and Safranin O b. (1: tibia, 2: femur). Arrows indicate increased inflammatory cells. (scale bar: 100 μ m) D. Blood IL-1 β levels in the non-RA and RA groups. (pg/ml) In the RA group, the IL- β concentration was 24.5 (pg/ml) * $P < 0.05$.

Fig 3.

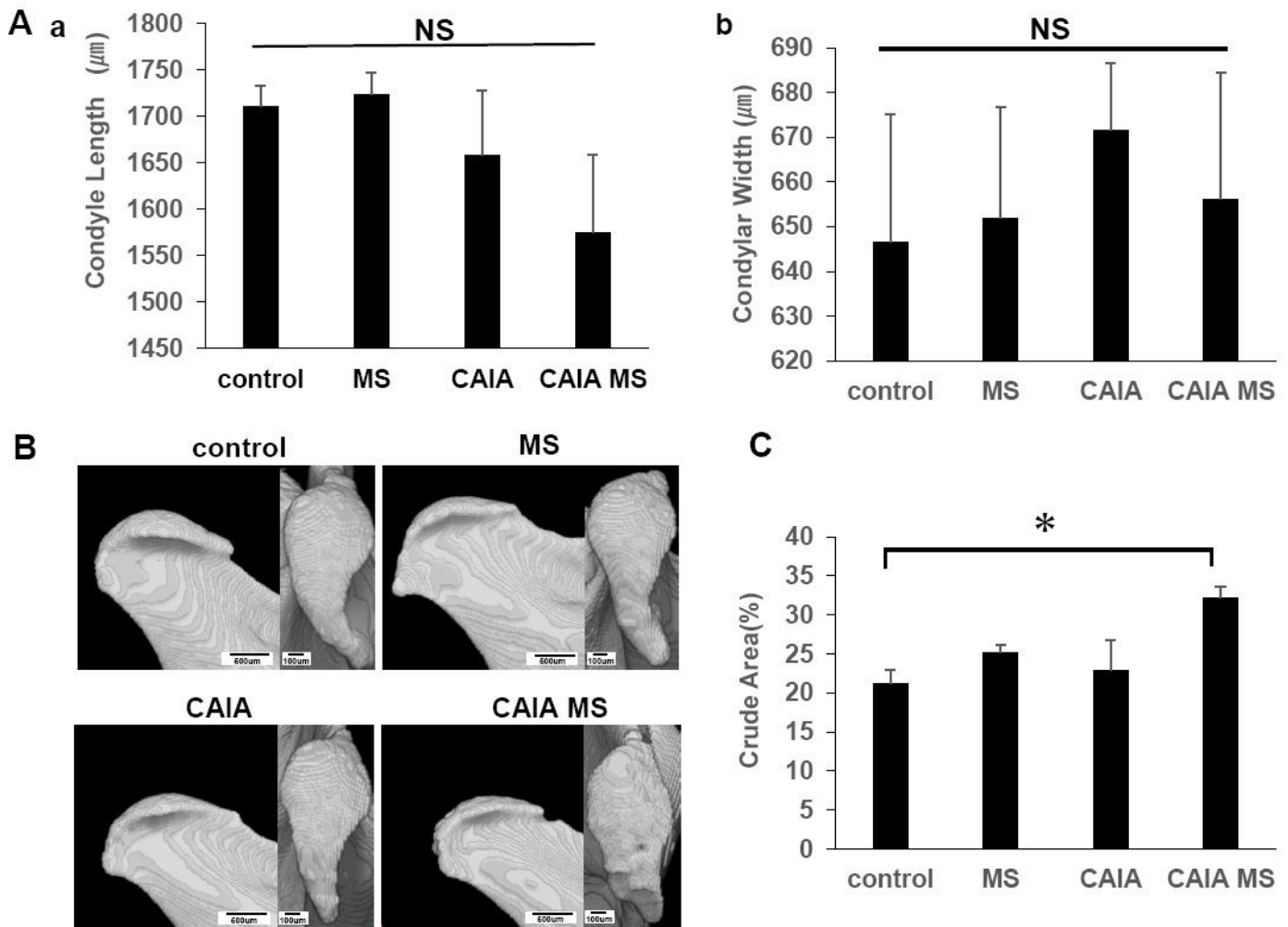


Figure 3

Evaluation of mandibular condyle morphology in micro-CT. A. a Mandibular condyle length of each group; b Mandibular condyle width of each group. There was no significant difference in change in either. B. Mandibular condyle lateral (scale bar: 500 μm) and superior (scale bar: 100 μm) morphology of each group. Red arrow indicates crude area. C. Percentage of crude area mandibular condyle in each group. The crude area was larger in the CAIA MS group. * $P < 0.05$.

Fig 4.

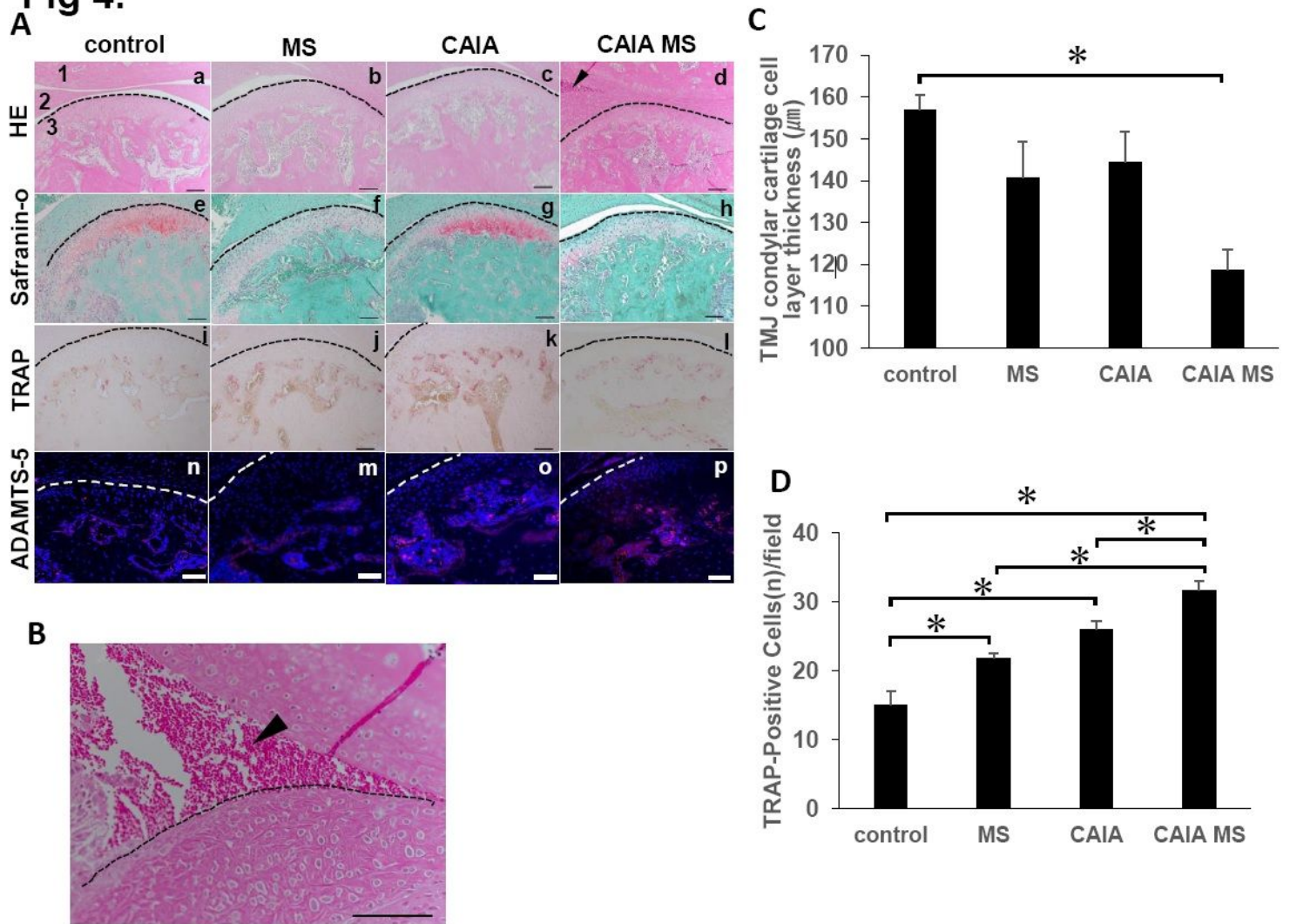


Figure 4

Histological evaluation of mandibular condyle morphology. A. (a–d) Representative hematoxylin and eosin staining with histological examination performed in each experimental group. Arrow indicates areas of inflammatory cell accumulation (1: mandibular fossa, 2: articular disc, 3: mandibular condyle). No major bone loss or other changes were observed. (e–h) Representative Safranin O staining. The Safranin O staining property is reduced by the addition of mechanical stress. (i–l) Representative TRAP staining. (n–p) Expression of ADAMTS-5 in the mandibular condyle (scale bar: 100 µm; red: ADAMTS-5, blue: cell nuclei). Enzyme localization in the chondrocyte layer was observed in all groups. B. Inflammatory cell accumulation findings in the superior articular space of the temporomandibular joint in the CAIA MS group. Arrow indicates area of inflammatory cell accumulation. (scale bar: 100 µm) C. TMJ cartilage cell layer thickness diameter assessment by HE staining. * P < 0.05. D. Number of TRAP-positive osteoclasts. The number of cells with three or more nuclei within a fixed measurement frame (450 µm × 900 µm) was counted. The CAIA MS group showed an average of 31.6 cells. * P < 0.05

Fig 5.

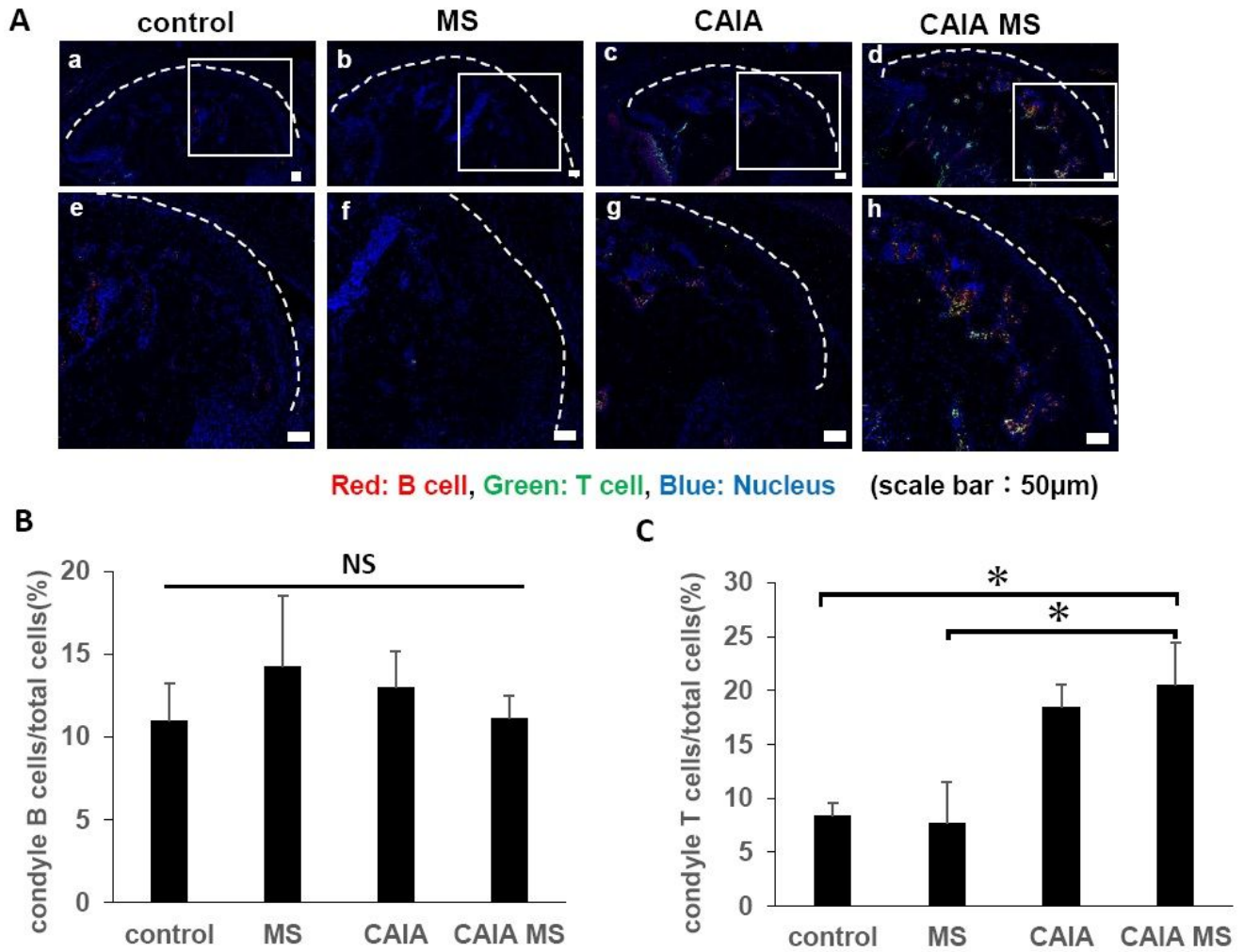


Figure 5

Localization of T cells and B cells in the mandibular condyle by immunofluorescence staining. A. Localization of mandibular condyle B cells and T cells (a–d) low magnification, and (e–h) high magnification. (scale bar: 50 μm; red: B cells, green: T cells, blue: cell nuclei). T cells and B cells are localized in the subchondral bone of each group. B. Number of B cells in the mandibular condyle vs. the total number of cells (percentage). * $P < 0.05$ C. Number of T cells in the mandibular condyle vs. the total number of cells (percentage). * $P < 0.05$

Fig 6.

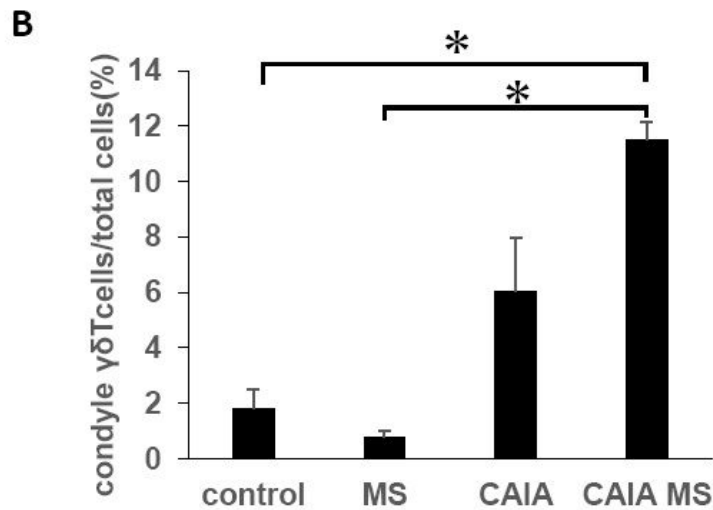
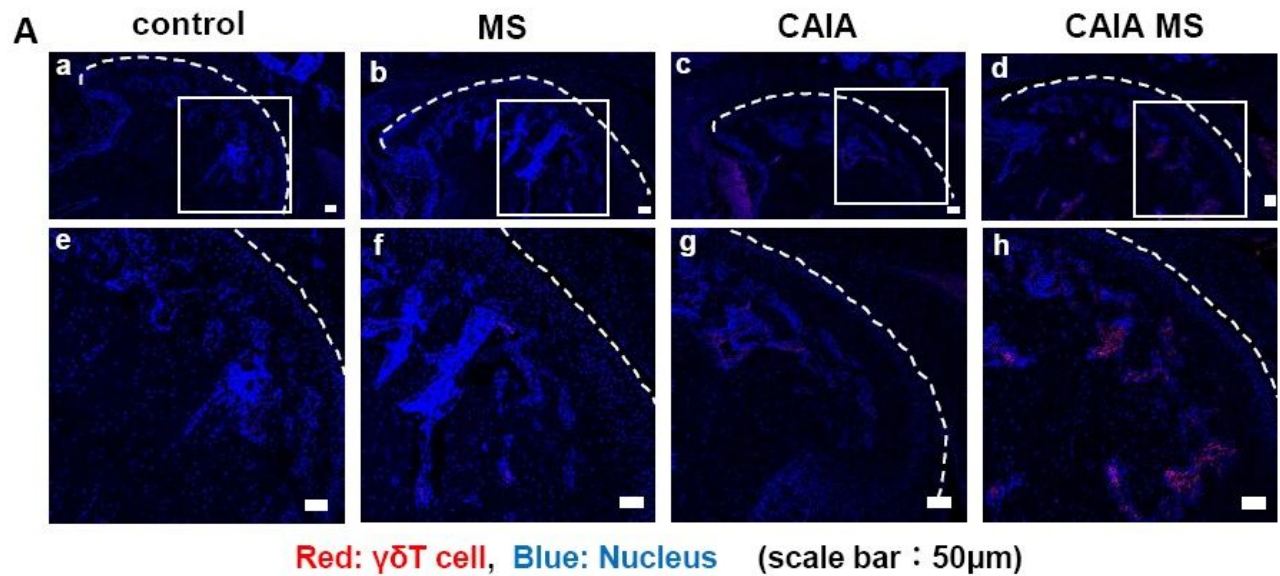


Figure 6

Localization of $\gamma\delta$ T cells in mandibular condyle by immunofluorescence staining. A. Localization of mandibular condyle $\gamma\delta$ T cells (a–d) Low magnification, and (e–h) high magnification. (scale bar: 50 μ m; red: $\gamma\delta$ T cells, blue: cell nuclei) $\gamma\delta$ T cells are localized in the subchondral bone of the CAIA MS group. B. Number of $\gamma\delta$ T cells in the mandibular condyle vs. the total number of cells (percentage). * $P < 0.05$